Title

Propanol Amination over Supported Nickel Catalysts: Reaction Mechanism and Role of the Support

Journal

ACS Catalysis, 9(4)

ISSN

2155-5435

Authors

Ho, CR
Defalque, V
Zheng, S
et al.

Publication Date

2019-04-05

DOI

10.1021/acscatal.8b04612

Peer reviewed

ACS Catalysis

Research Article

Cite This: ACS Catal. 2019, 9, 2931−2939

pubs.acs.org/acscatalysis

Propanol Amination over Supported Nickel Catalysts: Reaction Mechanism and Role of the Support

Christopher R. Ho,[†,‡] Vincent Defalque,[†] Steven Zheng,[†] and Alexis T. Bell*[,†,‡]

[†]Department of Chemical and Biomolecular Engineering, University of California, Berkeley, California 94720-1462, United States

[‡]Chemical Sciences Division, Lawrence Berkeley National Laboratory, Berkeley, California 94720, United States

Supporting Information

ABSTRACT: Ni-supported hydroxyapatite catalyst (Ni/HAP) was characterized and evaluated for propanol amination to propylamine at 423 K. The reaction proceeds via dehydroamination, a process that involves sequential dehydrogenation, condensation, and hydrogenation. Kinetic and isotopic studies indicate that α-H abstraction from propoxide species limits the rate of the dehydrogenation step and hence the overall rate of reaction. The rate of propanol dehydrogenation depends on the composition of the support and on the concentration of Ni sites located at the interface between Ni nanoparticles and the support. Ni/HAP is an order of magnitude more active than Ni/SiO_2 and displays a higher selectivity toward the primary amine. The superior performance of Ni/HAP is attributed to the high density of basic sites on HAP, which are responsible for stabilizing alkoxide intermediates and suppressing the disproportionation and secondary amination of amines.

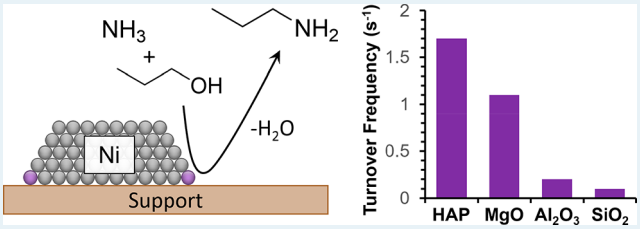

KEYWORDS: *hydroxyapatite, HAP, dehydroamination, alkylation, C−N coupling*

INTRODUCTION

Alkylamines are valuable precursors for many rubbers, herbicides, and pharmaceuticals and are typically produced by the amination of alcohols with ammonia.[1,2] Although this reaction can be performed over solid acid catalysts, the process requires high temperatures (573−773 K) and can lead to the formation of unwanted side products, such as olefins.[2,3] An alternative approach is to use a catalyst that dehydrogenates the alcohol to the corresponding alkanal. The alkanal then reacts with ammonia to form the alkylimine, which is then hydrogenated to the alkylamine. Suitable catalysts for this approach are Ni, Cu, Co, Pt, and Pd supported on a metal oxide.[4−12] These catalysts can operate at lower temperatures (373−623 K) as a result of the higher reactivity of the alkanal compared to that of the corresponding alcohol. Ni-containing catalysts in particular are promising because they exhibit high activity and stability for a variety of alcohols.[7,13−15]

A number of supports for Ni have been investigated for alcohol amination. These include SiO_2, Al_2O_3, CeO_x, La_2O_3, ZrO_2, TiO_2, and combinations thereof; however, the role of the support remains unclear.[7,9,11−16] Šolcová et al. have evaluated Ni supported on SiO_2, Al_2O_3, ZrO_2, TiO_2, and Nb_2O_5 and have found that the rates of diethylene glycol amination to diethlyene glycol amine varied only with the number of surface Ni sites, independent of support composition.[15] On the basis of these results, they concluded that the support affects the Ni dispersion but does not play a direct role in the reaction. On the other hand, Shimizu et al. have found that the support has a significant effect on the rate of 2-octanol amination with NH_3.[7] Of the catalysts tested, Ni/γ-Al_2O_3 was the most active. However, the reported turnover frequencies were based on the total number of Ni atoms instead of the number of surface Ni atoms, which makes the comparison of the intrinsic rates unclear. In a later study of 1-octanol amination with aniline over Ni/Al_2O_3, Shimizu et al. determined that the amination rate per surface Ni atom decreases with increasing Ni particle size, which suggests that Ni atoms located on the corners or edges of the nanoparticles are more active.[17] Cho et al. have studied 2-propanol amination with NH_3 over a series of Ni/Al_2O_3 catalysts with different alumina phases.[18] They observed that 2-propanol conversion increases with decreasing particle size, even though no clear trend was found between 2-propanol conversion and the Ni surface area. Large variations in monoisopropylamine selectivity were observed, which was attributed to differences in Lewis acid site densities of the alumina supports.

We have previously shown that hydroxyapatite (HAP) is an active catalyst for the Guerbet reaction of ethanol, which follows a mechanism similar to that proposed for alcohol amination.[19] This suggests that HAP would be an excellent support for the Ni-catalyzed amination of alkylamines. The present work was undertaken with the aim of elucidating the mechanism and kinetics of alcohol amination over Ni/HAP and the role of the support composition. To this end, we synthesized and characterized Ni/HAP and compared its activity to Ni/SiO_2 for a series of Ni particle sizes. The results

Received: November 16, 2018
Revised: January 17, 2019
Published: February 21, 2019

DOI: 10.1021/acscatal.8b04612
ACS Catal. 2019, 9, 2931−2939

show that for a given Ni surface area and particle size, Ni/HAP is significantly more active than Ni/SiO_2. We propose that the active site is located at the interface between the Ni nanoparticles and the support. The support does not affect the activation barrier for the rate-limiting step, α-H abstraction from a propoxide group, but instead is responsible for the formation of surface alkoxides, which are key intermediates in the reaction.

EXPERIMENTAL METHODS

Catalyst Synthesis. SiO_2 (Silicycle) and MgO (Sigma-Aldrich) were used without further treatment. Hydroxyapatite (HAP) was synthesized using a modification of the procedure reported by Tsuchida et al.[20] and Hanspal et al.[21] Aqueous solutions of 0.25 M $Ca(NO_3)_2{\cdot}4H_2O$ and 0.55 M $(NH_4)_2HPO_4$ were prepared and brought to a pH of 11 by the addition of ammonium hydroxide. The calcium solution was added dropwise to the phosphorus solution at room temperature and stirred for 0.5 h before heating to 353 K for an additional 3 h. The resulting slurry was filtered and washed with DI water. γ-Al_2O_3 was synthesized by calcining boehmite (Süd-Chemie) at 100 mL min^{-1} in air at 823 K for 3 h.

Ni-supported catalysts were prepared by incipient wetness impregnation using an aqueous solution of $Ni(NO_3)_2{\cdot}6H_2O$ on a support that had been dried at 393 K for 1 h. After impregnation, the sample was dried at 298 K overnight and subsequently calcined at 100 mL min^{-1} in air at 823 K for 2 h. All Ni-supported catalysts contain 4 wt % nickel unless otherwise specified.

Dipropylimine was synthesized by stirring stoichiometric amounts of propanol and propylamine at 298 K. After 5 min, K_2CO_3 was added to adsorb water and drive the reaction to completion. The product was extracted by centrifugation and stored for later use.

Characterization Techniques. Powder X-ray diffraction (PXRD) patterns were acquired with a Bruker D8 GADDS diffractometer equipped with a Cu Kα source (40 kV, 40 mA). BET surface areas were calculated from nitrogen adsorption isotherms obtained using a Micromeritics Gemini VII 2390 surface area analyzer after degassing the catalyst overnight at 393 K. Raman spectra were obtained using a LabRam HR Horiba Jobin Yvon spectrometer equipped with a 532 nm laser. Elemental compositions were measured by Galbraith Laboratories (Knoxville, TN) using ICP−OES.

Ni reducibility was measured with H_2 temperature-programmed reduction (TPR) using a Micromeritics AutoChem II 2920 instrument equipped with a thermal conductivity detector (TCD). Samples were pretreated under a flow of He at 823 K for 1 h before cooling to 313 K. Catalyst reduction was performed by flowing 4% H_2/Ar (50 mL min^{-1}) and raising the temperature from 313 to 973 K at 10 K min^{-1}. For H_2-TPR of Ni/HAP, the TCD response due to CO_2 desorption from bulk HAP was corrected for by using the H_2-TPR spectra of HAP as a reference. Elemental maps of Ni/HAP were obtained using an FEI Quanta FEG 250 scanning electron microscope (SEM) equipped with a Bruker Quantax energy-dispersive X-ray spectrometer (EDXS).

Static chemisorption of H_2 was performed using a Micromeritics 3 flex chemisorption analyzer. Samples were evacuated at 383 K for 0.5 h and then reduced in H_2 at the chosen reduction temperature (823 K unless otherwise specified) for 0.5 h. After evacuation at 723 K for 1 h, the samples were cooled to 313 K to measure the adsorption isotherm. Afterward, the samples were evacuated at 313 K for 1 h, and a subsequent isotherm was obtained to quantify the amount of weakly bound H_2. The total amount of chemisorbed H_2 was determined by taking the difference between the two isotherms. O_2 titration was performed by evacuating the same sample at 723 K for 0.5 h and pulsing in O_2 at 723 K. A Ni site density of 0.0677 nm^2/atom and adsorption stoichiometry of $1H/1Ni_{surface}$ were used to calculate the Ni surface area.[22] The average crystallite size was determined by assuming a spherical crystallite geometry.[22]

Measurements of Catalytic Activity. Measurements of reaction rates were carried out using a quartz-tube, packed-bed reactor (10 mm inner diameter). Quartz wool was placed below the catalyst bed to hold the catalyst in place. The reactor temperature was maintained using a tube furnace equipped with a Watlow temperature controller and a K-type thermocouple. Prior to reaction, the catalyst was treated at 30 mL min^{-1} in H_2 at the chosen reduction temperature (823 K unless otherwise specified) for 0.5 h before cooling to the reaction temperature.

In a typical experiment, propanol was introduced into a stream of He, H_2, and NH_3 using a syringe pump (World Precision Instruments, SP100I). Other liquid reactants were also fed in a similar manner. All experiments were carried out at atmospheric pressure. Product streams were analyzed by gas chromatography using an Agilent 6890A GC fitted with a HP-5 capillary column (30 m × 0.32 mm × 0.25 μm) and a flame ionization detector. Measurements of the rate of propanol amination were carried out at <10% conversion, where the only products observed were propylamine, dipropylamine, and tripropylamine. The reported amination rates were calculated by assuming that dipropylamine and tripropylamine are formed by the amination of 2 and 3 equiv of propanol, respectively.

Theoretical Calculations. Calculations of the thermodynamics of selected gas-phase reactions were carried out using the Q-Chem simulation package.[23] Optimization and frequency calculations were performed at the ωB97X-D/6-31G** level of theory, while single-point calculations were performed at the ωB97X-D/6-311++G(3df,3pd) level of theory.

RESULTS AND DISCUSSION

Characterization of IE-HAP Catalysts. The synthesized HAP support has a Ca/P ratio of 1.66 as determined by elemental analysis, which is consistent with a stoichiometric composition ($Ca_5(PO_4)_3OH$). The BET surface areas of HAP and Ni/HAP are 91 and 77 m^2/g, respectively. PXRD patterns for HAP and Ni/HAP are shown in Figure 1. The diffraction

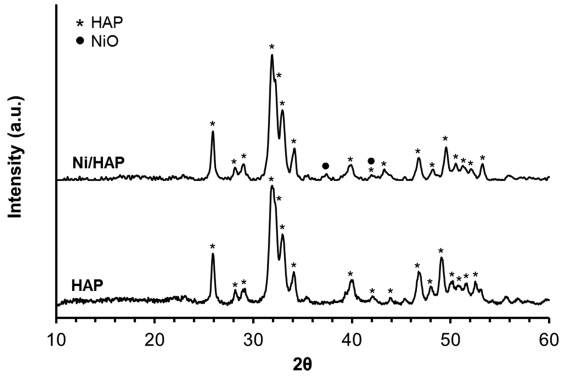

Figure 1. PXRD spectra of HAP and Ni/HAP.

DOI: 10.1021/acscatal.8b04612
ACS Catal. 2019, 9, 2931−2939

peaks associated with HAP are identical for both samples, indicating that the addition of nickel does not alter the crystal structure or lattice parameters of HAP. The HAP particle size is 21 nm for the bare support and 22 nm for Ni/HAP, as estimated by the Scherrer equation using the (002) diffraction peak. The weak diffraction peaks at 38 and 42° for Ni/HAP are characteristic of NiO, and the presence of NiO was verified by Raman spectroscopy (Figure S1). To gauge the reducibility of Ni species on HAP, H_2-TPR was performed (Figure 2). All

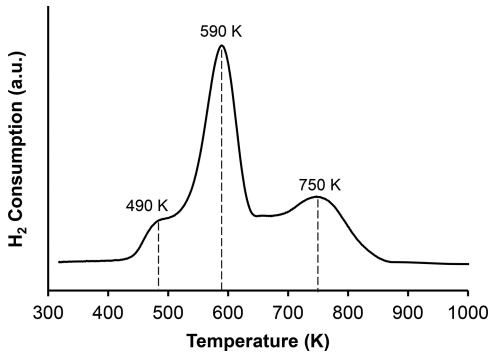

Figure 2. H_2-TPR spectra of Ni/HAP.

nickel was fully reduced by 850 K, assuming a 1:1 H_2/Ni reduction stoichiometry. The large reduction peak at 590 K corresponds to the reduction of bulk NiO species, while the shoulder peak at 490 K is due to the reduction of very small NiO particles.[24] The high-temperature peak at 750 K is indicative of the reduction of isolated Ni^{2+} species stabilized by the HAP framework, likely as a result of the substitution of two protons or Ca^{2+} in HAP by Ni^{2+}.[25]

Propanol Amination over Supported Ni Catalysts. HAP, Ni/HAP, Ni/SiO_2, Ni/Al_2O_3, and Ni/MgO were initially screened for propanol amination at 423 K (Scheme 1). All catalysts except the bare HAP support were active for the reaction, and the only products observed were propylamine **1**, dipropylamine **2**, and tripropylamine **3**. Ni-supported catalysts were inactive without H_2 pretreatment, showing that metallic Ni is necessary for the reaction to proceed. Ni/HAP was the most active catalyst tested, with a propanol conversion of 10.8% (Table 1). Ni/HAP also demonstrated a high selectivity toward propylamine (92%), with the major side product being dipropylamine. Ni/MgO was the least active catalyst with a conversion of 3.3%, while Ni/SiO_2 was the least selective toward propylamine. The differences in conversion and selectivity show that the support composition affects the catalytic activity.

A list of Ni-catalyzed amination rates for aliphatic alcohols has been compiled from the literature in Table S3. A direct comparison of rates is difficult because different authors used different reactants and reaction conditions. However, for the reaction of low-molecular-weight aliphatic alcohols at similar temperatures, the Ni/HAP catalyst demonstrates a higher TOF than other catalysts reported in the literature. We note, however, that Table 1 clearly shows that under identical reaction conditions and dispersions of Ni, the TOF for propanol amination is an order of magnitude higher for Ni/HAP than for Ni/Al_2O_3.

Mechanism of Propanol Amination over Ni/HAP. To understand the role of the support, it is first necessary to establish the reaction mechanism of propanol amination over Ni/HAP. Previous studies have shown that alcohol amination over Ni/SiO_2 and Ni/Al_2O_3 proceeds via a dehydroamination pathway, which involves sequential dehydrogenation, C−N coupling, and hydrogenation steps (Scheme 2).[7,13,26] For aliphatic alcohols, the initial dehydrogenation step has been reported to be rate-limiting.[4,5] An alternative pathway involves the direct coupling of alcohol and ammonia in one step, which occurs over solid acid catalysts such as zeolites.[27] One key difference between the two pathways is that hydroamination requires an alcohol reactant with an α-H for the initial dehydrogenation step. To determine which pathway occurs over Ni/HAP, the amination of *tert*-butanol was investigated. Prior work has shown that *tert*-butanol will readily couple with NH_3 via direct amination but not through dehydroamination because *tert*-butanol lacks an α-proton necessary to undergoing dehydrogenation.[27] When *tert*-butanol and NH_3 were fed over 4%Ni/HAP at 423 K under flowing H_2, no products were formed (Table S1), suggesting that direct amination does not occur over Ni/HAP. The mechanism was further probed by feeding NH_3 and H_2 with propanal, which is an intermediate in the dehydroamination pathway. Propanal was converted quantitatively to propylamine (Table S1), indicating that the amination of propanol follows a dehydroamination pathway. Moreover, the rapid rate of propanal conversion indicates that the initial dehydrogenation step is slow, consistent with previous literature reports for Ni-supported catalysts.[17]

Kinetic isotope experiments with ethanol were performed to verify the pathway and shed more light on the reaction mechanism. The rate of reaction was unaffected when H_2/ethanol was replaced with D_2/ethanol-D1 (Table S2), showing that the dissociation of H_2 and the cleavage of the O−H bond in propanol are not rate-limiting. However, a kinetic isotope effect (KIE) was observed when D_2/ethanol-D6 was used (k_H/k_D = 1.5). This result is in agreement with prior studies suggesting that α-H abstraction is rate-limiting in the dehydrogenation step. The magnitude of the KIE is similar to what Baiker et al. have reported for octanol amination over Cu/Al_2O_3.[5]

The dependences of the rate of propanol amination on reactant partial pressures are shown in Figures 3 and 4. The amination rate is positive order with respect to propanol at low propanol partial pressures and approaches zeroth order with increasing propanol partial pressures for the range of partial pressures tested (P_{PrOH} = 0.2−1.0 kPa). In contrast, the rate is zeroth order with respect to NH_3 for all NH_3 partial pressures

Scheme 1. Propanol Amination to Primary, Secondary, and Tertiary Amines

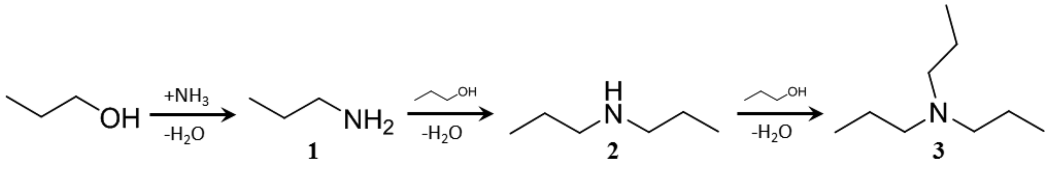

DOI: 10.1021/acscatal.8b04612
ACS Catal. 2019, 9, 2931−2939

Table 1. Propanol Amination with NH_3 over Nickel-Supported Catalysts[a]

catalyst	Ni particle size (nm)	Ni dispersion[b]	Ni surface area (m^2/g)[c]	conversion (%)	TOF (s^{-1})[d]	selectivity (%)		
						1	2	3
HAP				~0				
Ni/HAP	16.5	0.042	3.9	10.8	1.7	92	8	<1
Ni/MgO	10.4	0.014	0.3	3.3	1.1	84	16	<1
Ni/SiO_2	6.3	0.065	1.6	4.4	0.1	74	24	2
$Ni/\gamma\text{-}Al_2O_3$	4.9	0.041	1.0	4.5	0.2	88	12	<1

[a]Reaction conditions: T = 423 K; catalyst mass = 0.02 g; $P_{propanol}$ = 1 kPa; P_{NH_3} = 5 kPa; P_{H_2} = 95 kPa; total gas flow rate at STP = 30 mL min^{-1} [b]Dispersion defined as the number of surface Ni^0 atoms over the total loading of Ni. [c]Based on H_2 chemisorption and O_2 titration measurements. [d]Turnover frequencies (TOF) defined as the rates per perimeter Ni atom as determined by H_2 chemisorption and O_2 titration.

Scheme 2. Hydroamination Pathway for Propanol Amination to Propylamine

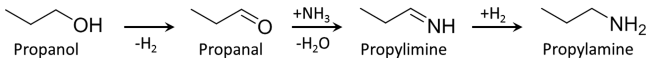

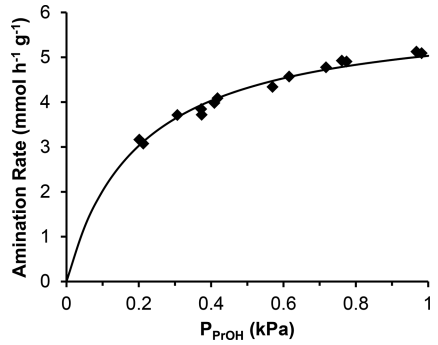

Figure 3. Effect of propanol partial pressure on amination rate. Reaction conditions: T = 423 K, Ni/HAP = 0.02 g, P_{NH_3} = 5 kPa, P_{H_2} = 95 kPa, and total gas flow rate at STP = 60 mL min^{-1}.

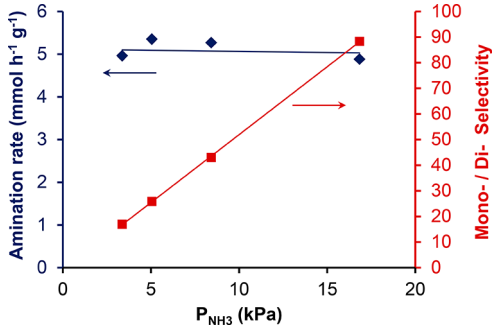

Figure 4. Effect of NH_3 partial pressure on the propanol amination rate and selectivity of propylamine vs dipropylamine. Reaction conditions: T = 423 K, Ni/HAP = 0.01 g, $P_{propanol}$ = 1 kPa, P_{H_2} = 83–96 kPa, and total gas flow rate at STP = 30 mL min^{-1}.

tested (3.4–16.8 kPa). The results suggest that the sites responsible for propanol dehydrogenation are predominantly empty or are occupied by propanol-derived species. NH_3 has been proposed to aid in alcohol dehydrogenation over the Ni(111) surface.[28] However, the rate over Ni/HAP does not vary with NH_3 partial pressure. Thus, an NH_3-mediated pathway may not be relevant for supported Ni catalysts.

As seen in Figure 4, the ratio of the production of propylamine to dipropylamine shows a strong dependence on the NH_3 partial pressure. This finding is consistent with the proposed mechanism in which a propanal intermediate can react with either NH_3 to form propylamine or with propylamine to form dipropylamine. One interesting question is whether C–N bond formation takes place in the gas phase or on the surface. Several groups have reported that the C–N coupling reaction in the liquid phase is facile and can occur spontaneously in solution, while others have hypothesized that the reaction takes place on the catalyst surface based on the observation of a dependence of the product selectivity on catalyst composition.[29,30] To probe for C–N coupling in the gas phase, propanal and propylamine were fed through a blank reactor. Quantitative conversion to dipropylimine was observed, showing that the reaction does not require a catalyst (Table S1). However, when a similar experiment was conducted with propanal and ammonia, no products were formed (Table S1). Primary imines are known to be unstable, so the lack of reaction could be due to the inherent thermodynamics instead of a kinetic limitation. Gas-phase DFT calculations reveal that the Gibbs free energy of reaction, ΔG_{rxn}, for propanal and NH_3 to form propylimine is +33 kJ/mol while the ΔG_{rxn} for the reaction of propanal and propylamine to form dipropylimine is −0.6 kJ/mol (Scheme S1). The subsequent hydrogenation of propylimine (ΔG_{rxn} = −62 kJ/mol) or dipropylimine (ΔG_{rxn} = −39 kJ/mol) is highly favorable. On the basis of these Gibbs free energy calculations, the equilibrium conversion of propanal and NH_3 to propylimine is approximately 1%. It is therefore tempting to suggest that the coupling of propanal and NH_3 requires a catalyst because no propylimine was detected in the product stream. However, we cannot rule out the possibility that small amounts of propylimine are formed but hidden beneath the propanal signal in the chromatogram because the retention time of propylimine only could be estimated due to the lack of a stable propylimine standard.

The amination rate and product selectivity are invariant with the H_2 partial pressure for P_{H_2} = 5–95 kPa (Figure S2). However, the catalyst is quickly deactivated if H_2 is not present because of the formation of metal nitrides and carbonaceous species.[8,11,31] Although H_2 does not play a direct role in the dehydrogenation reaction, a small amount is necessary to keep the Ni nanoparticles in their active metallic state. Possible product inhibition was investigated by cofeeding H_2O, butanal (as a proxy for propanal), diethylamine (as a proxy for dipropylamine), or triethylamine (as a proxy for tripropylamine). In all cases, no significant change in the reaction rate was observed, indicating that none of the above products or intermediates compete with propanol for the active site. (Figure S3).

Role of Support in Propanol Amination over Ni Catalysts. To gain more insight into the site requirements and

DOI: 10.1021/acscatal.8b04612
ACS Catal. 2019, 9, 2931–2939

role of the support, a series of Ni/HAP and Ni/SiO_2 catalysts with different Ni particle sizes were synthesized by varying the metal loading and reduction temperature (Table 2). Larger Ni particles were obtained at higher Ni loadings and higher reduction temperatures. Propanol amination rates were measured for all catalysts and are shown in Figure 5. When the rates are normalized by the number of surface Ni atoms, the rates decrease with increasing Ni particle size, suggesting that the Ni atoms located at the edges or corners are the active sites. Shimizu et al. have reported a similar observation for cyclodecanol dehydrogenation over Ni/θ-Al_2O_3.[32] An alternative hypothesis is that the support plays a direct role in alcohol dehydrogenation, in which case the active sites would be Ni perimeter sites located at the interface of the metal and the support. This would explain why Ni/HAP is more active than Ni/SiO_2 for a given particle size. The number of perimeter Ni particles was determined by assuming the Ni nanoparticle has the shape of a truncated cuboctahedron and then calculating the number of perimeter sites based on the nanoparticle size and number of Ni surface sites, as demonstrated by Cargnello et al.[33] Note that because the particle surface area is proportional to the square of a characteristic radius and the particle perimeter is proportional to its radius, the relationships among perimeter sites, surface sites, and particle size should be similar for various particle geometries. When the rates are normalized by the number of perimeter Ni sites (Figure 5b), the turnover frequencies become invariant with particle size, suggesting that the Ni perimeter sites are the ones active for propanol dehydrogenation.

Table 2. Synthesis Conditions and Characterization of Ni/HAP and Ni/SiO_2 Catalysts

catalyst	Ni loading (wt %)[a]	reduction temperature (K)	Ni surface area (m^2/g)[b]	fraction of Ni reduced (%)[b]	Ni particle size (nm)[a]
Ni/HAP-8.3	4.02	623	2.2	69	8.3
Ni/HAP-9.9	4.02	673	2.3	82	9.9
Ni/HAP-13.0	4.02	723	2.0	95	13.0
Ni/HAP-16.5 (Ni/HAP)	4.02	823	1.6	99	16.5
Ni/SiO_2-6.3 (Ni/SiO_2)	3.95	823	3.9	93	6.3
Ni/SiO_2-7.6	3.95	923	3.4	97	7.6
Ni/SiO_2-12.5	11.3	823	6.7	98	12.5
Ni/SiO_2-16.6	22.9	823	8.8	94	16.6

[a]From ICP-OES conducted by Galbraith Laboratories. [b]Based on H_2 chemisorption and O_2 titration measurements.

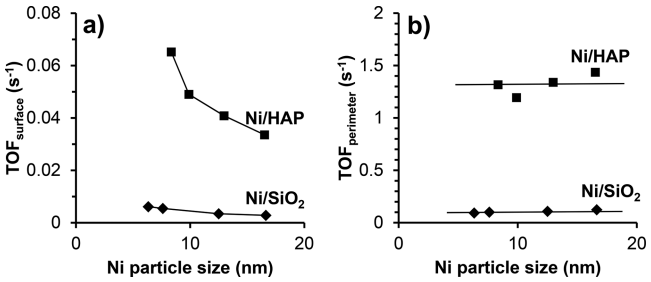

Figure 5. Effect of support and Ni particle size on turnover frequencies (TOF) of propanol amination. (a) TOF is based on the number of surface Ni sites. (b) TOF is based on the number of perimeter Ni sites. Reaction conditions: T = 423 K, $mass_{catalyst}$ = 0.02 g, $P_{propanol}$ = 1 kPa, P_{NH_3} = 5 kPa, P_{H_2} = 95 kPa, and total gas flow rate at STP = 60 mL min^{-1}.

To determine why the support affects the reaction rates, it is helpful to construct a plausible mechanism for propanol dehydrogenation over Ni/HAP (Scheme 3). The adsorption of propanol and the formation of the corresponding propoxide are facile over HAP, suggesting that gas-phase propanol (I), molecularly adsorbed propanol (II), and surface propoxide (III) are in pseudoequilibrium with each other.[34] The subsequent rate-limiting α-H abstraction occurs on a neighboring Ni site (IV) because dehydrogenation does not proceed in the absence of Ni at 423 K. Recombination of the surface hydrogen atoms (V) and desorption of the products complete the catalytic cycle.

An alternative mechanism is that dehydrogenation takes place exclusively on Ni, and the support serves only to modify the electronic properties of the metal. In this case, the activation barrier for α-H abstraction would depend on the nature of the support. To test this possibility, the activation energy was measured over Ni/HAP-16.5 and Ni/SiO_2-12.5 at P_{PrOH} = 2.0 kPa, where all interfacial sites are covered predominantly with propanol-derived surface species (Figures S4 and S5). As shown in Figure 6, the activation energies over both catalysts are similar ($E_{a,Ni/HAP}$ = 68 kJ/mol; $E_{a,Ni/SiO_2}$ = 70 kJ/mol), indicating that the support does not affect the electronic properties of the Ni nanoparticles and hence the rate of the α-H abstraction step. Instead, the difference in turnover frequencies between Ni/HAP and Ni/SiO_2 suggests that the properties of the support affect the concentration of the active surface propoxide species. Several groups have shown that alcohol adsorption on SiO_2 leads mainly to molecularly adsorbed alcohol, and only a small fraction of surface species are alkoxides which form by the condensation of alcohol/silanol groups or the opening of the siloxane bridges.[35−37] On the other hand, HAP is known to have a high density of basic sites that can activate alcohols.[21,38] This is evident when looking at the adsorption microcalorimetry of ethanol. The differential heat of ethanol adsorption over HAP ($\Delta H_{EtOH} \approx$ 100 kJ/mol) remains constant up to a surface coverage of 4 μmol m^{-2}, which is indicative of a surface that contains strongly chemisorbed ethanol species.[21] For SiO_2, the differential heat of ethanol adsorption decreases rapidly from ~100 to ~60 kJ mol^{-1} as the surface coverage increases to 1 μmol m^{-2}, consistent with the idea that most alcohols on SiO_2 are weakly bound, physisorbed species.[35] Shimuzu et al. have proposed a similar role for the support in 2-propanol dehydrogenation over Ni/Al_2O_3.[32] On the basis of catalyst screening and FTIR studies, the group hypothesized that the basic sites in θ-Al_2O_3 were responsible for the formation of 2-propoxide species.[32] This conclusion parallels that drawn from studies of alcohol amination carried out with homogeneous catalysts in which alcohol dehydrogenation and amination over metal complexes typically require the addition of a base such as

DOI: 10.1021/acscatal.8b04612
ACS Catal. 2019, 9, 2931−2939

Scheme 3. Proposed Reaction Mechanism for Propanol Dehydrogenation over Ni/HAP

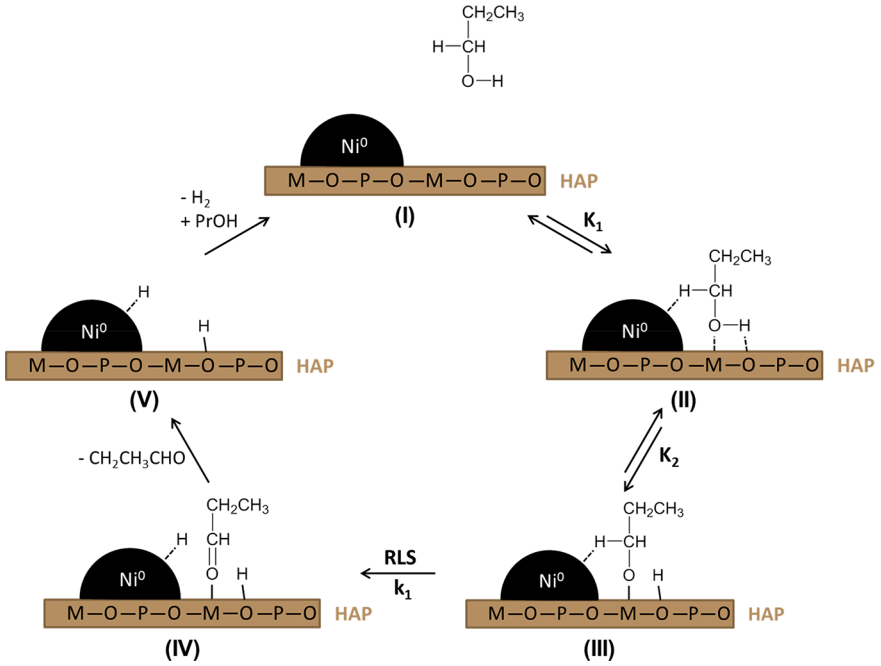

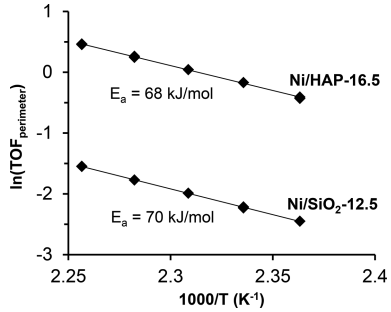

Figure 6. Arrhenius plots of propanol amination over Ni/HAP-16.5 and Ni/SiO_2-12.5. Reaction conditions: T = 423 K, $mass_{catalyst}$ = 0.02 g, $P_{propanol}$ = 1 kPa, P_{NH_3} = 5 kPa, P_{H_2} = 95 kPa, and total gas flow rate at STP = 60 mL min^{-1}.

K_2CO_3 to deprotonate the alcohol and form the alkoxide.[39,40] Although MgO is a basic support that can catalyze alkoxide formation, the Ni/MgO catalyst exhibited a lower TOF than did Ni/HAP (Table 1). This is likely due to the higher density of base sites on the HAP support, which translates to a higher concentration of propoxide species on the surface and hence to a higher TOF even after normalizing the rates per perimeter Ni atom.[21]

An additional factor that could explain the large difference in activity between Ni/HAP and Ni/SiO_2 is the ability of Ni/HAP to catalyze hydrogen-transfer reactions because HAP is known to be active for hydrogen-transfer reactions between alcohols and aldehydes.[19,41−43] These hydrogen-transfer reactions are rapid in comparison to dehydrogenation and can accelerate condensation rates by providing an alternate pathway for producing aldehydes.[19] To determine whether Ni/HAP is active for hydrogen transfer between alcohols and imines, propanol and dipropylimine were fed to the reactor. No dipropylamine was observed in the product stream, indicating that hydrogen transfer to a C═N bond is much more difficult than the corresponding reaction over the more polar C═O bond.

Space−time studies over Ni/HAP and Ni/SiO_2 were performed to evaluate the effect of the support in product selectivity. For both catalysts, propylamine selectivity decreased and dipropylamine selectivity increased with increasing propanol conversion, as shown in Figure 7. This is consistent

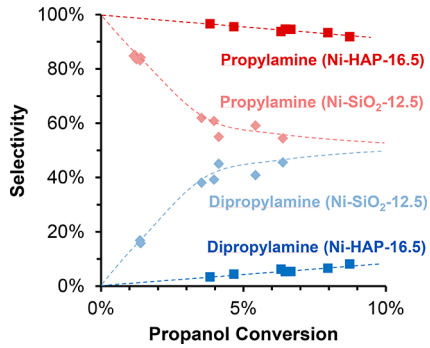

Figure 7. Space−time studies showing the selectivity of propylamine and dipropylamine as a function of propanol conversion over Ni/HAP-16.5 and Ni/SiO_2-12.5. Reaction conditions: T = 423 K, $mass_{catalyst}$ = 0.02 g, $P_{propanol}$ = 1 kPa, P_{NH_3} = 5 kPa, and P_{H_2} = 95 kPa.

with a mechanism in which propylamine is a primary product that can react further to form dipropylamine. There are two main pathways for dipropylamine formation. One pathway is a consecutive amination reaction, wherein propylamine and propanol react to give dipropylamine and water. The other pathway is the disproportionation of 2 equiv of propylamine to give dipropylamine and NH_3. For a given propanol conversion, Ni/HAP is more selective toward propylamine than Ni/SiO_2.

To determine whether this difference in selectivity is due to differences in secondary amination or disproportion rates, experiments with ethanol/NH_3/propylamine feeds were performed to decouple the amination and disproportion

DOI: 10.1021/acscatal.8b04612
ACS Catal. 2019, 9, 2931−2939

rates. Primary amination of ethanol yields ethylamine, secondary amination of ethanol yields ethylpropylamine, and the disproportionation of propylamine yields dipropylamine (Scheme 4). The disproportion rate was 3 times higher over

Scheme 4. Possible Amination and Disproportionation Reactions for an Ethanol/NH_3/Propylamine Feed

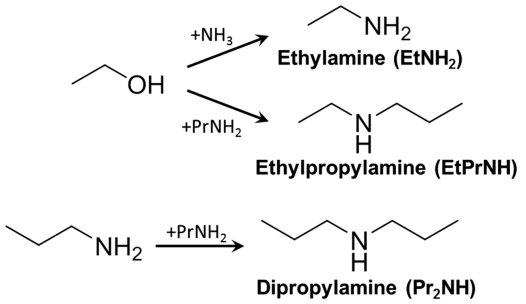

Ni/SiO_2 than over Ni/HAP, which partially explains why Ni/HAP is more selective for the primary amine than Ni/SiO_2 (Table 3). The reason for the low disproportion rates over Ni/

Table 3. Disproportionation of Propylamine over Ni/HAP-16.5 and Ni/SiO_2-12.5[a]

	formation rate (mmol h^{-1} g_{cat}^{-1})		
catalyst	ethylamine	ethylpropylamine	dipropylamine
Ni/HAP-16.5	1.90	1.39	0.62
Ni/SiO_2-12.5	0.69	1.50	1.79

[a]Reaction conditions: T = 423 K, $mass_{catalyst}$ = 0.01 g, P_{PrOH} = 0.1 kPa, $P_{ethylamine}$ = 0.1 kPa, P_{NH_3} = 5 kPa, P_{H_2} = 95 kPa, and total gas flow rate at STP = 30 mL min^{-1}.

HAP is likely due to a lack of strong Lewis acid sites, which are known to be active for disproportionation.[31] The small fraction of unreduced Ni in Ni/SiO_2 can lead to the generation of Lewis acid sites, and Verhaak et al. have demonstrated that Ni/SiO_2 is an active catalyst for disproportionation.[31]

The relative rates of primary and secondary amination also depend on the support. Ethylamine and ethylpropylamine are both formed from a common ethanal intermediate, and the ratio of their formation rates is proportional to the ratio of NH_3 and propylamine partial pressures. This is illustrated in eq 1, where k represents a rate constant, P represents the partial pressure, and $[CH_3CHO^*]$ represents the surface concentration of propanal on the support. This expression is consistent with the observed trends in product selectivities and in the NH_3 kinetics of propanol amination (Figure 4).

$$\frac{r_{EtNH_2}}{r_{EtPrNH}} = \frac{k_{EtNH_2}P_{EtNH_2}[CH_3CHO^*]}{k_{EtPrNH}P_{EtPrNH}[CH_3CHO^*]} \quad (1)$$

The coupling of ethanal is more facile with propylamine than with NH_3 because propylamine is a stronger nucleophile and secondary imines are more stable than primary imines. The ratio of rate constants for ethanal coupling with propylamine vs NH_3 $\left(\frac{k_{EtPrNH}}{k_{EtNH_2}}\right)$ is 37 over Ni/HAP and 109 over Ni/SiO_2. The different rate constants for the two catalysts indicate that the support plays an important role in the condensation step. Furthermore, this is evidence that C−N coupling occurs on the support surface and not exclusively in the gas phase. We hypothesize that $\frac{k_{EtPrNH}}{k_{EtNH_2}}$ is higher over Ni/HAP because of the basic nature of the HAP support, which lowers the effective concentration of adsorbed propylamine compared to that of SiO_2. Thus, Ni/HAP is more selective toward the primary amine than Ni/SiO_2 because both the secondary amination and disproportionation reactions are suppressed more greatly over HAP.

One question that arises is whether the density of active Ni sites affects the product selectivity. Propanol amination with propylamine has the same mechanism and site requirements as propanol amination with NH_3, so the number of active Ni sites should not affect the relative selectivity of these two reactions as long as the results are compared at isoconversion. However, the density of active Ni sites could affect the relative rate of amination and disproportionation.

While a detailed mechanistic understanding of amine disproportionation is outside the scope of this work, it has been generally proposed that disproportionation occurs in a three-step process that involves the dehydrogenation of the propylamine to propylimine, the coupling of propylimine with another propylamine, and the hydrogenation of the resulting secondary imine to form dipropylamine.[4,31] Starting from a propylimine intermediate, hydrogenation would yield propylamine, while disproportionation would yield dipropylamine. Thus, the density of active Ni sites could affect the rate of propylimine hydrogenation, which would impact product selectivity.

To investigate this possibility, the selectivity to propylamine at a given propanol conversion (~10% for Ni/HAP, ~3.5% for Ni/SiO_2) was plotted as a function of the number of Ni perimeter sites for all supported Ni catalysts (Figure S7). The selectivity to propylamine appears to be invariant with the number of perimeter Ni sites for a given support. To explain this result, we note that the disproportionation of propylamine occurs under certain reaction conditions (Table 3), indicating that propylamine dehydrogenation to propylimine is a relevant process. Thus, increasing the density of Ni sites will increase the rates of both propylimine hydrogenation and propylamine dehydrogenation, which would explain why the density of Ni perimeter sites does not significantly affect product selectivity (Scheme S2).

However, for a catalyst with a low density of active Ni sites, increasing the number of Ni sites could lead to an increase in selectivity. For example, basic 4% Ni/MgO exhibits a lower selectivity to propylamine than does acidic 4% Ni/Al_2O_3. This appears to contradict the idea that Lewis acid supports are more active for disproportionation and secondary amination. However, a close inspection of the 4% Ni/MgO catalyst reveals that only 14% of Ni is reduced after treatment in H_2 at 773 K. This is due to the difficulty of reducing Ni on a MgO support. The 4% Ni/MgO catalyst has fewer active Ni sites compared to 4% Ni/Al_2O_3 (0.3 vs 2.2 $\mu mol/g_{cat}$). In addition, the unreduced NiO on MgO can serve as Lewis acid sites. These two factors could explain why Ni/MgO has a lower selectivity to propylamine than does 4% Ni/Al_2O_3.

To test this hypothesis, a 12% Ni/MgO catalyst was synthesized by an impregnation method. Compared to 4%Ni/MgO, the 12% Ni/MgO catalyst has a higher Ni loading and larger NiO particles, which results in a higher fraction of reduced Ni after H_2 treatment. As a result, the 12% Ni/MgO catalyst has more active Ni sites and fewer Lewis acid sites than 4% Ni/MgO, which should lead to an increase in propylamine

DOI: 10.1021/acscatal.8b04612
ACS Catal. 2019, 9, 2931−2939

selectivity. Indeed, at a conversion of ~3.5%, the propylamine selectivity over 12% Ni/MgO (89%, Table S1) was higher than that of 4% Ni/MgO (84%). Thus, the propylamine selectivity can be improved by increasing the number of Ni sites and decreasing the number of Lewis acid sites. Unfortunately, the contribution due to the two effects could not be decoupled. A similar trend has been observed by Cabello et al. over Ni/hydrotalcite, where the Ni reducibility and support basicity depend on the Ni and Mg loadings.[44] For a more comprehensive review of support effects on selectivity, the authors refer to Gomez et al.[30]

CONCLUSIONS

We have demonstrated that Ni/HAP is an active catalyst for propanol amination to propylamine. The reaction proceeds through a dehydroamination pathway and is limited by the rate of α-H abstraction from propanol. The turnover frequency for this reaction is invariant with Ni particle size when normalized by the number of perimeter Ni atoms, suggesting that the active sites for dehydrogenation are located at the interface between the metal and the support. Ni/HAP is more active and selective toward the primary amine than Ni/SiO_2, highlighting the importance of the support. Although Ni is solely responsible for the α-H abstraction step, the support affects the reaction rate by deprotonating the alcohol to form active alkoxide intermediates. The subsequent coupling of propanal with ammonia is rapid and quantitative, independent of the ammonia partial pressure. While propylimine formed by this reaction is thermodynamically unstable, its rapid hydrogenation over the Ni nanoparticles leads to the thermodynamically favorable formation of propylamine. Experimental evidence suggests that the reaction of propanal with ammonia occurs on the surface of HAP, whereas the hydrogenation of propylimine occurs on the surface of the Ni nanoparticles (Scheme 5). The secondary reaction of product propylamine

Scheme 5. Proposed Reaction Mechanism for Propanol Amination over Ni/HAP

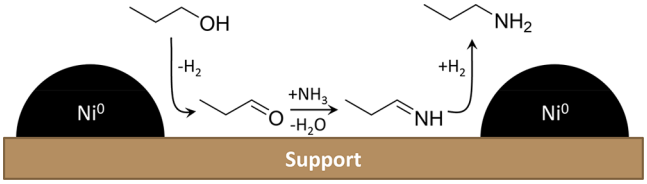

with propanal to form dipropylamine also occurs on the surface of HAP but is increasingly suppressed as the partial pressure of ammonia is increased. This secondary reaction occurs to a much lower degree over Ni/HAP than over Ni/SiO_2. Finally, we have found that the disproportionation of propylamine to dipropylamine and ammonia is disfavored over Ni/HAP compared to Ni/SiO_2.

ASSOCIATED CONTENT

Supporting Information

The Supporting Information is available free of charge on the ACS Publications website at DOI: 10.1021/acscatal.8b04612.

Raman spectra and EDX analysis of Ni/HAP, additional catalytic testing, KIE studies, DFT calculated gas-phase enthalpies and free energies of reactions, and a comparison of TOF values with the literature (PDF)

AUTHOR INFORMATION

Corresponding Author

*E-mail: bell@cchem.berkeley.edu.

ORCID

Alexis T. Bell: 0000-0002-5738-4645

Notes

The authors declare no competing financial interest.

ACKNOWLEDGMENTS

This work was funded by the Director, Office of Science, Office of Basic Energy Sciences of the U.S. Department of Energy under contract no. DE-AC02-05CH11231. DFT calculations were performed on a computing cluster sponsored by the National Institutes of Health (NIH S10OD023532). The authors thank Darinka Primc for assistance with EDX measurements and Sankaranaryanapillai Shylesh, Neelay Phadke, and Julie Rorrer for helpful discussions.

REFERENCES

(1) Roose, P.; Eller, K.; Henkes, E.; Rossbacher, R.; Höke, H. *Amines, Aliphatic*, 5th ed.; Wiley-VCH: Weinheim, 2015.
(2) Hayes, K. S. Industrial Processes for Manufacturing Amines. *Appl. Catal., A* **2001**, *221*, 187−195.
(3) Veefkind, V. A.; Lercher, J. A. On the Elementary Steps of Acid Zeolite Catalyzed Animation of Light Alcohols. *Appl. Catal., A* **1999**, *181*, 245−255.
(4) Baiker, A.; Kijenski, J. Catalytic Synthesis of Higher Aliphatic Amines from the Corresponding Alcohols. *Catal. Rev.: Sci. Eng.* **1985**, *27*, 653−697.
(5) Baiker, A.; Caprez, W.; Holstein, W. L. Catalytic Amination of Aliphatic Alcohols in the Gas and Liquid Phases: Kinetics and Reaction Pathway. *Ind. Eng. Chem. Prod. Res. Dev.* **1983**, *22*, 217−225.
(6) Corma, A.; Ródenas, T.; Sabater, M. J. A Bifunctional PdVMgO Solid Catalyst for the One-Pot Selective N-Monoalkylation of Amines with Alcohols. *Chem. - Eur. J.* **2010**, *16*, 254−260.
(7) Shimizu, K.; Kon, K.; Onodera, W.; Yamazaki, H.; Kondo, J. N. Heterogeneous Ni Catalyst for Direct Synthesis of Primary Amines from Alcohols and Ammonia. *ACS Catal.* **2013**, *3*, 112−117.
(8) Rausch, A. K.; van Steen, E.; Roessner, F. New Aspects for Heterogeneous Cobalt-Catalyzed Hydroamination of Ethanol. *J. Catal.* **2008**, *253*, 111−118.
(9) Sewell, G.; O'Connor, C.; van Steen, E. Reductive Amination of Ethanol with Silica-Supported Cobalt and Nickel Catalysts. *Appl. Catal., A* **1995**, *125*, 99−112.
(10) Furukawa, S.; Suzuki, R.; Komatsu, T. Selective Activation of Alcohols in the Presence of Reactive Amines over Intermetallic PdZn: Efficient Catalysis for Alcohol-Based N-Alkylation of Various Amines. *ACS Catal.* **2016**, *6*, 5946−5953.
(11) Cho, J. H.; Park, J. H.; Chang, T.-S.; Seo, G.; Shin, C.-H. Reductive Amination of 2-Propanol to Monoisopropylamine over Co/γ-Al2O3 Catalysts. *Appl. Catal., A* **2012**, *417*−*418*, 313−319.
(12) Li, S.; Wen, M.; Chen, H.; Ni, Z.; Xu, J.; Shen, J. Amination of Isopropanol to Isopropylamine over a Highly Basic and Active Ni/LaAlSiO Catalyst. *J. Catal.* **2017**, *350*, 141−148.
(13) Bassili, V. a.; Baiker, A. Catalytic Amination of 1-Methoxy-2-Propanol Silica Supported Nickel over Study of the Influence of the Reaction Parameters. *Appl. Catal.* **1990**, *65*, 293−308.
(14) Fischer, A.; Mallat, T.; Baiker, A. Amination of Diols and Polyols to Acyclic Amines. *Catal. Today* **1997**, *37*, 167−189.
(15) Šolcová, O.; Jirátová, K. Role of the Support of the Nickel Catalyst in the Synthesis of Morpholine from Diethylene Glycol and Ammonia. *J. Mol. Catal.* **1994**, *88*, 193−203.
(16) Shimizu, K.; Kanno, S.; Kon, K.; Hakim Siddiki, S. M. A.; Tanaka, H.; Sakata, Y. N-Alkylation of Ammonia and Amines with Alcohols Catalyzed by Ni-Loaded CaSiO3. *Catal. Today* **2014**, *232*, 134−138.

DOI: 10.1021/acscatal.8b04612
ACS Catal. 2019, 9, 2931−2939

(17) Shimizu, K.; Imaiida, N.; Kon, K.; Hakim Siddiki, S. M. A.; Satsuma, A. Heterogeneous Ni Catalysts for N-Alkylation of Amines with Alcohols. *ACS Catal.* **2013**, *3*, 998−1005.
(18) Cho, J. H.; An, S. H.; Chang, T. S.; Shin, C. H. Effect of an Alumina Phase on the Reductive Amination of 2-Propanol to Monoisopropylamine over Ni/Al2O3. *Catal. Lett.* **2016**, *146*, 811−819.
(19) Ho, C. R.; Shylesh, S.; Bell, A. T. Mechanism and Kinetics of Ethanol Coupling to Butanol over Hydroxyapatite. *ACS Catal.* **2016**, *6*, 939−948.
(20) Tsuchida, T.; Kubo, J.; Yoshioka, T.; Sakuma, S.; Takeguchi, T.; Ueda, W. Reaction of Ethanol over Hydroxyapatite Affected by Ca/P Ratio of Catalyst. *J. Catal.* **2008**, *259*, 183−189.
(21) Hanspal, S.; Young, Z. D.; Shou, H.; Davis, R. J. Multiproduct Steady-State Isotopic Transient Kinetic Analysis of the Ethanol Coupling Reaction over Hydroxyapatite and Magnesia. *ACS Catal.* **2015**, *5*, 1737−1746.
(22) Bartholomew, C. H.; Pannell, R. B. The Stoichiometry of Hydrogen and Carbon Monoxide Chemisorption on Alumina- and Silica-Supported Nickel. *J. Catal.* **1980**, *65*, 390−401.
(23) Shao, Y.; Gan, Z.; Epifanovsky, E.; Gilbert, A. T. B.; Wormit, M.; Kussmann, J.; Lange, A. W.; Behn, A.; Deng, J.; Feng, X.; Ghosh, D.; Goldey, M.; Horn, P. R.; Jacobson, L. D.; Kaliman, I.; Khaliullin, R. Z.; Kuš, T.; Landau, A.; Liu, J.; Proynov, E. I.; Rhee, Y. M.; Richard, R. M.; Rohrdanz, M. a.; Steele, R. P.; Sundstrom, E. J.; Woodcock, H. L.; Zimmerman, P. M.; Zuev, D.; Albrecht, B.; Alguire, E.; Austin, B.; Beran, G. J. O.; Bernard, Y. a.; Berquist, E.; Brandhorst, K.; Bravaya, K. B.; Brown, S. T.; Casanova, D.; Chang, C. M.; Chen, Y.; Chien, S. H.; Closser, K. D.; Crittenden, D. L.; Diedenhofen, M.; Distasio, R. a.; Do, H.; Dutoi, A. D.; Edgar, R. G.; Fatehi, S.; Fusti-Molnar, L.; Ghysels, A.; Golubeva-Zadorozhnaya, A.; Gomes, J.; Hanson-Heine, M. W. D.; Harbach, P. H. P.; Hauser, A. W.; Hohenstein, E. G.; Holden, Z. C.; Jagau, T. C.; Ji, H.; Kaduk, B.; Khistyaev, K.; Kim, J.; Kim, J.; King, R. a.; Klunzinger, P.; Kosenkov, D.; Kowalczyk, T.; Krauter, C. M.; Lao, K. U.; Laurent, A. D.; Lawler, K. V.; Levchenko, S. V.; Lin, C. Y.; Liu, F.; Livshits, E.; Lochan, R. C.; Luenser, A.; Manohar, P.; Manzer, S. F.; Mao, S. P.; Mardirossian, N.; Marenich, A. V.; Maurer, S. a.; Mayhall, N. J.; Neuscamman, E.; Oana, C. M.; Olivares-Amaya, R.; Oneill, D. P.; Parkhill, J. a.; Perrine, T. M.; Peverati, R.; Prociuk, A.; Rehn, D. R.; Rosta, E.; Russ, N. J.; Sharada, S. M.; Sharma, S.; Small, D. W.; Sodt, A.; Stein, T.; Stück, D.; Su, Y. C.; Thom, A. J. W.; Tsuchimochi, T.; Vanovschi, V.; Vogt, L.; Vydrov, O.; Wang, T.; Watson, M. a.; Wenzel, J.; White, A.; Williams, C. F.; Yang, J.; Yeganeh, S.; Yost, S. R.; You, Z. Q.; Zhang, I. Y.; Zhang, X.; Zhao, Y.; Brooks, B. R.; Chan, G. K. L.; Chipman, D. M.; Cramer, C. J.; Goddard, W. a.; Gordon, M. S.; Hehre, W. J.; Klamt, A.; Schaefer, H. F.; Schmidt, M. W.; Sherrill, C. D.; Truhlar, D. G.; Warshel, A.; Xu, X.; Aspuru-Guzik, A.; Baer, R.; Bell, A. T.; Besley, N. a.; Chai, J. Da; Dreuw, A.; Dunietz, B. D.; Furlani, T. R.; Gwaltney, S. R.; Hsu, C. P.; Jung, Y.; Kong, J.; Lambrecht, D. S.; Liang, W.; Ochsenfeld, C.; Rassolov, V. a.; Slipchenko, L. V.; Subotnik, J. E.; Van Voorhis, T.; Herbert, J. M.; Krylov, A. I.; Gill, P. M. W.; Head-Gordon, M. Advances in Molecular Quantum Chemistry Contained in the Q-Chem 4 Program Package. *Mol. Phys.* **2015**, *113*, 184−215.
(24) Miniach, E.; Śliwak, A.; Moyseowicz, A.; Gryglewicz, G. Growth of Carbon Nanofibers from Methane on a Hydroxyapatite-Supported Nickel Catalyst. *J. Mater. Sci.* **2016**, *51*, 5367−5376.
(25) Jun, J. H.; Lee, T. J.; Lim, T. H.; Nam, S. W.; Hong, S. A.; Yoon, K. J. Nickel-Calcium Phosphate/Hydroxyapatite Catalysts for Partial Oxidation of Methane to Syngas: Characterization and Activation. *J. Catal.* **2004**, *221*, 178−190.
(26) Cho, J. H.; Park, J. H.; Chang, T. S.; Kim, J. E.; Shin, C. H. Reductive Amination of 2-Propanol to Monoisopropylamine over Ni/γ-Al2O3 Catalysts. *Catal. Lett.* **2013**, *143*, 1319−1327.
(27) Huang, M.; Wang, Q.; Yi, X.; Chu, Y.; Dai, W.; Li, L.; Zheng, A.; Deng, F. Insight into the Formation of the Tert-Butyl Cation Confined inside H-ZSM-5 Zeolite from NMR Spectroscopy and DFT Calculations. *Chem. Commun.* **2016**, *52*, 10606−10608.
(28) Dumon, A. S.; Wang, T.; Ibañez, J.; Tomer, A.; Yan, Z.; Wischert, R.; Sautet, P.; Pera-Titus, M.; Michel, C. Direct: N-Octanol Amination by Ammonia on Supported Ni and Pd Catalysts: Activity Is Enhanced by "Spectator" Ammonia Adsorbates. *Catal. Sci. Technol.* **2018**, *8*, 611−621.
(29) Heinen, A. W.; Peters, J. A.; van Bekkum, H. The Reductive Amination of Benzaldehyde over Pd/C Catalysts: Mechanism and Effect of Carbon Modifications on the Selectivity. *Eur. J. Org. Chem.* **2000**, *2000* (13), 2501−2506.
(30) Gomez, S.; Peters, J. A.; Maschmeyer, T. The Reductive Animation of Aldehydes and Ketones and the Hydrogenation of Nitriles: Mechanistic Aspects and Selectivity Control. *Adv. Synth. Catal.* **2002**, *344*, 1037−1057.
(31) Verhaak, M. J. F. M.; van Dillen, A. J.; Geus, J. W. Disproportionation of N-Propylamine on Supported Nickel Catalysts. *Appl. Catal., A* **1994**, *109*, 263−275.
(32) Shimizu, K. I.; Kon, K.; Shimura, K.; Hakim, S. S. M. a. Acceptor-Free Dehydrogenation of Secondary Alcohols by Heterogeneous Cooperative Catalysis between Ni Nanoparticles and Acid-Base Sites of Alumina Supports. *J. Catal.* **2013**, *300*, 242−250.
(33) Cargnello, M.; Doan-Nguyen, V. V. T.; Gordon, T. R.; Diaz, R. E.; Stach, E. a.; Gorte, R. J.; Fornasiero, P.; Murray, C. B. Control of Metal Nanocrystal Size Reveals Metal-Support Interface Role for Ceria Catalysts. *Science (Washington, DC, U. S.)* **2013**, *341*, 771−773.
(34) Kibby, C. L.; Hall, W. Dehydrogenation of Alcohols and Hydrogen Transfer from Alcohols to Ketones over Hydroxyapatite Catalysts. *J. Catal.* **1973**, *31*, 65−73.
(35) Natal-Santiago, M. A.; Dumesic, J. A. Microcalorimetric, FTIR, and DFT Studies of the Adsorption of Methanol, Ethanol, and 2,2,2-Trifluoroethanol on Silica. *J. Catal.* **1998**, *175*, 252−268.
(36) Luts, T.; Katz, A. Chemisorption and Dehydration of Ethanol on Silica: Effect of Temperature on Selectivity. *Top. Catal.* **2012**, *55*, 84−92.
(37) Barnette, A. L.; Asay, D. B.; Janik, M. J.; Kim, S. H. Adsorption Isotherm and Orientation of Alcohols on Hydrophilic SiO2 under Ambient Conditions. *J. Phys. Chem. C* **2009**, *113*, 10632−10641.
(38) Tsuchida, T.; Sakuma, S.; Takeguchi, T.; Ueda, W. Direct Synthesis of N-Butanol from Ethanol over Nonstoichiometric Hydroxyapatite. *Ind. Eng. Chem. Res.* **2006**, *45*, 8634−8642.
(39) Dobereiner, G. E.; Crabtree, R. H. Dehydrogenation as a Substrate-Activating Strategy in Homogeneous Transition-Metal Catalysis. *Chem. Rev.* **2010**, *110*, 681−703.
(40) Almeida, M. L. S.; Beller, M.; Wang, G. Z.; Bäckvall, J. E. Ruthenium(II)-Catalyzed Oppenauer-Type Oxidation of Secondary Alcohols. *Chem. - Eur. J.* **1996**, *2*, 1533−1536.
(41) Ogo, S.; Onda, A.; Iwasa, Y.; Hara, K.; Fukuoka, A.; Yanagisawa, K. 1-Butanol Synthesis from Ethanol over Strontium Phosphate Hydroxyapatite Catalysts with Various Sr/P Ratios. *J. Catal.* **2012**, *296*, 24−30.
(42) Moteki, T.; Flaherty, D. W. Mechanistic Insight to C-C Bond Formation and Predictive Models for Cascade Reactions among Alcohols on Ca- and Sr-Hydroxyapatites. *ACS Catal.* **2016**, *6*, 4170−4183.
(43) Young, Z. D.; Davis, R. J. Hydrogen Transfer Reactions Relevant to Guerbet Coupling of Alcohols over Hydroxyapatite and Magnesium Oxide Catalysts. *Catal. Sci. Technol.* **2018**, *8*, 1722−1729.
(44) Cabello, F. M.; Tichit, D.; Coq, B.; Vaccari, A.; Dung, N. T. Hydrogenation of Acetonitrile on Nickel-Based Catalysts Prepared from Hydrotalcite-like Precursors. *J. Catal.* **1997**, *167*, 142−152.

DOI: 10.1021/acscatal.8b04612
ACS Catal. 2019, 9, 2931−2939